

# Geophysical Research Letters

## RESEARCH LETTER

10.1029/2019GL083237

### Key Points:

- Measurements made from 40 to 325 m above the Amazon Forest do not show evidence of an inertial sublayer
- The roughness sublayer directly merges with the mixed layer under daytime unstable conditions
- New methods and theories will be needed to address the nonexistence of the inertial sublayer to estimate fluxes over the Amazon forest

### Supporting Information:

- Supporting Information S1
- Data Set S1
- Data Set S2
- Data Set S3
- Data Set S4
- Data Set S5
- Data Set S6
- Data Set S7
- Data Set S8
- Data Set S9
- Data Set S10
- Data Set S11
- Data Set S12
- Data Set S13

### Correspondence to:

N. Luís Dias,  
nelsonluisdias@gmail.com

### Citation:

Dias-Júnior, C. Q., Luís Dias, N., dos Santos, R. M. N., Sörgel, M., Araújo, S., Tsokankunku, A., et al. (2019). Is there a classical inertial sublayer over the Amazon forest? *Geophysical Research Letters*, 46, 5614–5622. <https://doi.org/10.1029/2019GL083237>

Received 10 OCT 2018

Accepted 24 APR 2019

Accepted article online 30 APR 2019

Published online 30 MAY 2019

## Is There a Classical Inertial Sublayer Over the Amazon Forest?

Cléo Quaresma Dias-Júnior<sup>1</sup> , Nelson Luís Dias<sup>2</sup> , Rosa Maria N. dos Santos<sup>3</sup>, Matthias Sörgel<sup>4,5</sup>, Alessandro Araújo<sup>6</sup>, Anywhere Tsokankunku<sup>4,5</sup>, Florian Ditas<sup>7</sup> , Raoni Aquino de Santana<sup>8</sup>, Celso von Randow<sup>9</sup> , Marta Sá<sup>10</sup>, Christopher Pöhlker<sup>7</sup>, Luiz Augusto Toledo Machado<sup>9</sup> , Leonardo Deane de Sá<sup>9</sup>, Daniel Moran-Zuloaga<sup>7</sup>, Ruud Janssen<sup>1,11,12</sup> , Otávio Acevedo<sup>1,2,13</sup> , Pablo Oliveira<sup>1,2,13</sup>, Gilberto Fisch<sup>1,3,14</sup>, Tomas Chor<sup>1,4,15</sup> , and Antonio Manzi<sup>9</sup>

<sup>1</sup>Department of Physics, Federal Institute of Pará, Belém, Brazil, <sup>2</sup>Department of Environmental Engineering, Federal University of Paraná (UFPR), Curitiba, Brazil, <sup>3</sup>School of Technology, Meteorology, State University of Amazonas (UEA), Manaus, Brazil, <sup>4</sup>Biogeochemistry Department, Max Planck Institute for Chemistry, Mainz, Germany, <sup>5</sup>Now at the Atmospheric Chemistry Department, Max Planck Institute for Chemistry, Mainz, Germany, <sup>6</sup>Empresa Brasileira de Pesquisa Agropecuária (EMBRAPA), Belém, Brazil, <sup>7</sup>Multiphase Chemistry Department, Max Planck Institute for Chemistry, Mainz, Germany, <sup>8</sup>Institute of Engineering and Geosciences, Federal University of West Pará (UFOPA), Santarém, Brazil, <sup>9</sup>Instituto Nacional de Pesquisas Espaciais (INPE), Cachoeira Paulista, Brazil, <sup>10</sup>Large Scale Biosphere-Atmosphere Experiment in Amazonia (LBA), National Institute of Research of the Amazon (INPA), Manaus, Brazil, <sup>11</sup>Atmospheric Chemistry Department, Max Planck Institute for Chemistry, Mainz, Germany, <sup>12</sup>Now at the Department of Civil and Environmental Engineering, Massachusetts Institute of Technology, Cambridge, MA, USA, <sup>13</sup>Department of Physics, Federal University of Santa Maria (UFSM), Santa Maria, Brazil, <sup>14</sup>Divisão de Ciências Atmosféricas, Centro Técnico Aeroespacial, Instituto de Aeronáutica e Espaço, São José dos Campos, Brazil, <sup>15</sup>Department of Atmospheric and Oceanic Sciences, University of California, Los Angeles, CA, USA

**Abstract** On the basis of measurements over different surfaces, an inertial sublayer (ISL), where Monin-Obukhov Similarity Theory applies, exists above  $z = 3h$ , where  $h$  is canopy height. The roughness sublayer is within  $h < z < 3h$ . Most studies of the surface layer above forests, however, are able to probe only a narrow region above  $h$ . Therefore, direct verification of an ISL above tall forests is difficult. In this study we conducted a systematic analysis of unstable turbulence characteristics at heights from 40 to 325 m, measured at an 80m, and the recently built 325-m Amazon Tall Tower Observatory towers over the Amazon forest. Our analyses have revealed no indication of the existence of an ISL; instead, the roughness sublayer directly merges with the convective mixed layer above. Implications for estimates of momentum and scalar fluxes in numerical models and observational studies can be significant.

**Plain Language Summary** The Amazon forest interacts with the atmosphere by emitting and absorbing many substances, such as carbon dioxide, methane, ozone, and organic compounds, produced by the vegetation. These substances are very influential in both the regional and global climates, and until now, the estimates of their emission and absorption rates are based on classical theories developed originally over relatively short vegetation and valid for a region above the ground called the “inertial sublayer.” In this work we present evidence, obtained with the help of measurements from a very tall tower (325 m), that a classical inertial sublayer does not exist over the Amazon forest. New methods to quantify the emission and absorption rates, therefore, will be needed to improve their estimates.

## 1. Introduction

Recent assessments of the roughness sublayer (RSL) in unstable conditions at the Amazon Tall Tower Observatory (ATTO; see Andreae et al., 2015) site over the Amazon forest have shown that it extends to at least 80 m, the highest level where measurements were previously made (Chor et al., 2017; Zahn et al., 2016). With the completion of the 325-m-high ATTO main tower, it is now possible to measure considerably higher. A first set of micrometeorological simultaneous measurements was made during October–November 2015 at 40, 55, 81, 150, and 325 m, which presents a unique opportunity to explore some key questions to understand the exchanges between the forest and the atmosphere:

1. What height does the RSL reach?
2. Under unstable conditions, is there a typical inertial sublayer (ISL) above the RSL? Or does the RSL merge directly into mixed layer (ML) characteristics? (In this work, the surface layer [SL] is considered to be composed of the RSL and the ISL; Raupach & Thom, 1981).

If there is an ISL and measurements are made high enough, then Monin-Obukhov Similarity Theory (MOST), or some extension of it, can be used for long-term monitoring of scalar fluxes above the forest with methods like fluxgradient, scintillometric estimates, relaxed eddy accumulation, and Bowen ratio. Similar arguments apply to fluxes in boundary conditions of numerical models. This is important, because many studies regarding the estimation of scalar fluxes over the Amazon employ MOST although this is inappropriate (Kuhn et al., 2007; von Randow et al., 2006), because measurements are made inside the RSL (e.g., Alves et al., 2018; Chor et al., 2017). The impact on the errors in the estimated fluxes can be significant (see section 4.1), as well as on Large-Eddy Simulations (LES) simulations (Basu & Lacser, 2017).

It is possible, however, that a classical ISL does not exist (see Figure 5.1 of Malhi et al., 2004). In this case, efforts should be directed at developing theories both for the RSL and for the ML to provide the required flux estimates.

## 2. Site and Data

The study area is located at Reserva de Desenvolvimento Sustentável Uatumã, in the counties of São Sebastião do Uatumã and Itapiranga, in Amazonas State, Brazil. The site is 150km northeast of the state capital Manaus, between  $2^{\circ} 27' - 2^{\circ} 4' S$  and  $54^{\circ} 10' - 58^{\circ} 4' W$ . Since 2011, an 80-m scaffolding tower at the site has been used for measurements inside and above the canopy. During 2015, the main 325-m steel lattice tower was erected. They are 670 m apart. Tree height is in the range 30–40 m, with occasional patches of fallen trees.

A first intensive observation period at the tall tower during the dry season (IOP-1) was conducted during 25 October to 25 November 2015. Sonic anemometers were positioned at 40, 55, and 81 m (CSAT3, *Campbell Scientific Inc.*) on the 80-m tower. On the tall tower, anemometers were positioned at 150 (CSAT3) and 325 m (IRGASON, *Campbell Scientific Inc.*). Measurements at the 80-m tower were already in place before the IOP; this arrangement also avoids local effects from a clearing around the tall tower. It was not possible to intercompare the sonic anemometers, but they are considered to be accurate enough to allow estimates of velocity gradients (Chor et al., 2017). The 30-min measurement periods (“blocks”) when the wind was coming from behind the tower were discarded, avoiding flow distortion errors. Quality control procedures (Mauder & Foken, 2004; Vickers & Mahrt, 1997) were applied using EddyPro© (*LI-COR Inc.*, Lincoln, USA). Details on the data processing and data used are given in Supporting Information S1. Radiosoundings were launched (*GRW DFM09*) at a clearing 5km south, and a ceilometer (*Jenoptik CHM15k*) operated 400m southeast, of the ATTO tower.

## 3. The Approach to Identify the RSL, the ISL, and the ML

We evaluated data at the five levels of measurement and tested them both for MOST and for ML scaling. We expect both scalings to fail in the RSL. Analyses are of two types: (i) At each level  $z$ , we test turbulent standard deviations, horizontal heat fluxes, and dissipation rates for different scalings, and (ii) we test several statistics against  $z/z_i$ , where  $z_i$  is the height of the Atmospheric Boundary Layer (ABL).

From type-i analyses, we expect that for the lower levels, MOST should fail, because we are in the RSL; for intermediate levels, the success of MOST should increase (as we are approaching, or are inside, the ISL); finally, for the upper levels, MOST scaling should again fail as we are in the ML. Conversely, ML scaling should fail at the lower levels and produce increasingly better results at higher levels. In all cases, as  $z$  increases, three different patterns should emerge if there is an ISL but just two if only the RSL and the ML are present.

From type-ii analyses, a comprehensive view of the whole ABL should emerge: A three-tiered structure should be discernible if an ISL is present and a two-tiered one if only the RSL and the ML exist. Type-ii has difficulties, however, because (1) we are not aware of observational studies comprising the three layers; (2) separate identification of the RSL and the ISL is difficult in  $z/z_i$  coordinates; and (3) turbulence measure-

**Table 1**  
Error Statistics for Flux-Gradient Estimates at the Amazonas Tall Tower Observatory Site

Flux	Unit	Overall mean	Absolute RMSE	Relative RMSE	BIAS	<i>r</i>
<i>LE</i>	W/m <sup>2</sup>	211.70	201.58	1.34	-46.87	0.39
<i>F</i>	μmol · m <sup>-2</sup> · s <sup>-1</sup>	-0.357	0.615	65.21	0.033	0.16

Note. RMSE = root mean square error.

ments are scarce above the ISL, usually coming from aircraft and laboratory studies. Moreover, as the height of the ABL extends beyond 325 m in the middle of the day, there are fewer data at  $z/z_i \sim 1$ .

Friction velocity and virtual temperature turbulent scale are calculated from

$$u_*^2 = -\overline{u'w'}|_0, \quad u_*\vartheta_{v*} = \overline{w'\vartheta'_v}|_0, \quad (1)$$

where the subscript 0 indicates the 40-m level. In (1),  $u$  is the horizontal velocity (rotated into the mean wind),  $w$  the vertical velocity, and  $\vartheta_v$  is the virtual temperature; overbars and primes have the usual meaning.

The ML scales  $w_*$  and  $\vartheta_{v*}$  are

$$w_* = \left[ \frac{g}{\overline{\vartheta_v}} \overline{w'\vartheta'_v}|_0 z_i \right]^{1/3}, \quad w_*\vartheta_{v*} = \overline{w'\vartheta'_v}|_0, \quad (2)$$

where  $g = 9.81 \text{ m/s}^2$  and  $\overline{\vartheta_v}$  is measured at 40 m. The Obukhov length and stability parameter are

$$L_O = -\frac{u_*^2 \overline{\vartheta_v}}{\kappa g \vartheta_{v*}}, \quad \zeta = -\frac{z-d}{L_O}, \quad (3)$$

where  $\kappa = 0.40$ , with the displacement height  $d = 0.75h = 30 \text{ m}$ , where  $h = 40 \text{ m}$  is the canopy height.

## 4. Results

### 4.1. Errors in the Flux-Gradient Method

Flux-gradient methods have been assessed in a few studies over forests such as Mölder et al. (1999). For the Amazon, MOST dimensionless gradients have been obtained by Viswanadham et al. (1990) and more recently by Chor et al. (2017). Interestingly, however, results are not reported in terms of errors in the flux estimates. Therefore, we calculated error statistics using Chor et al.'s (2017) data to provide a quantitative estimate of the magnitude of the errors incurred by application of MOST in the RSL. Table 1 shows the absolute and relative root mean square errors, the bias, and the correlation coefficient  $r$  for the latent heat (*LE*) and  $\text{CO}_2$  (*F*) fluxes by MOST. Note that the dimensionless gradients have been corrected for the forest site. As it can be seen, the errors are substantial.

### 4.2. Height of the ABL

Reliable estimates of the height of the ABL (the height of the potential temperature inversion) are essential for ML scaling. Potential temperature profiles were measured in the first 6 days of IOP-1 with radiosondes. However, a ceilometer operated continuously, allowing simultaneously available data to be used to obtain a relationship between radiosonde and ceilometer-derived  $z_i$ .

The ceilometer measured mean 30-s backscatter profiles up to 4,500 m with 15-m resolution. An automatically calculated  $z_i$ , based on the vertical gradient of backscattered energy (Steyn et al., 1999), was used. The aerosol concentration is usually higher in the ML: a maximum in the gradient indicates  $z_i$ . This is a common method to calculate  $z_i$  from both ground-based and aircraft-borne instruments (Brooks, 2003; Melfi et al., 1985; Steyn et al., 1999; Sawyer & Li, 2013; Wang et al., 2012).

The results of the method were visually confirmed: In spite of the typical scatter in boundary-layer height estimates (Freire & Dias, 2013), the agreement was very good (see Supporting Information S1). The mean ABL heights are close to those found by Fisch et al. (2004) in Rondônia, Brazil. After that, a lag between the ceilometer and the radiosonde  $z_i$  was found, with the radiosonde values lagging 1 hr behind. Consequently, the ceilometer values were shifted back 1 hr to agree with the radiosonde. From here on, the  $z_i$  values used for the whole campaign are 30-min means from the ceilometer.

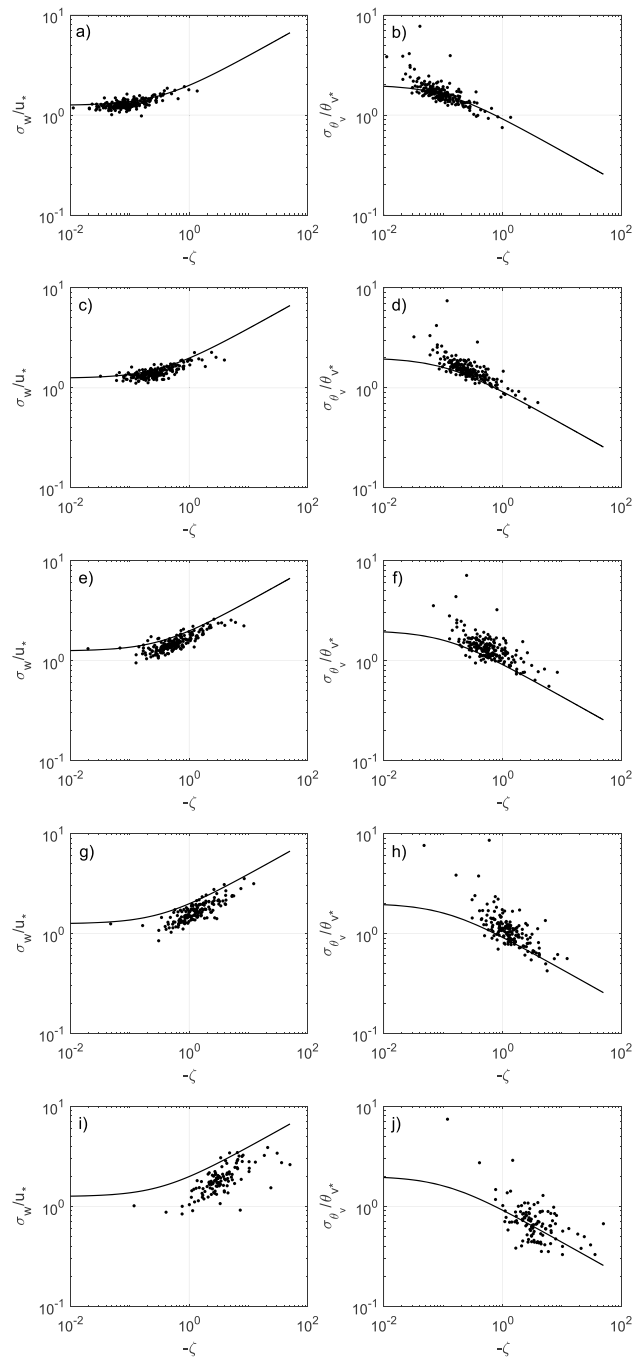


**Figure 1.**  $\sigma_w/u_*$  and  $\sigma_{\theta_v}/\theta_{v*}$  from measurements at 40 (a,b), 55 (c,d), 81 (e,f), 150 (g,h), and 325 m (i,j). The black lines show the Monin-Obukhov Similarity Theory functions from the literature.

### 4.3. Type-i Analysis: MOST Scaling

Figure 1 shows the nondimensional standard deviations  $\phi_w = \sigma_w/u_*$  and  $\phi_{\theta_v} = \sigma_{\theta_v}/\theta_{v*}$  as functions of  $\zeta$ . There is low scatter in  $\sigma_w/u_*$  and good agreement with the standard function for the ISL reported in the literature (equation (11), Chor et al., 2017) for the levels 40 m, 55 m, and slightly less so for 81 m (Figures 1a, 1c, and 1e). These results confirm the findings of Zahn et al. (2016) and Chor et al. (2017) for the same site. At the 150- and 325-m levels, the scatter is considerably larger than that observed at the lower levels (Figures 1g–1i). Note that the dimensionless velocity gradients  $\phi_\tau$  found by Chor et al. (2017) in the RSL are

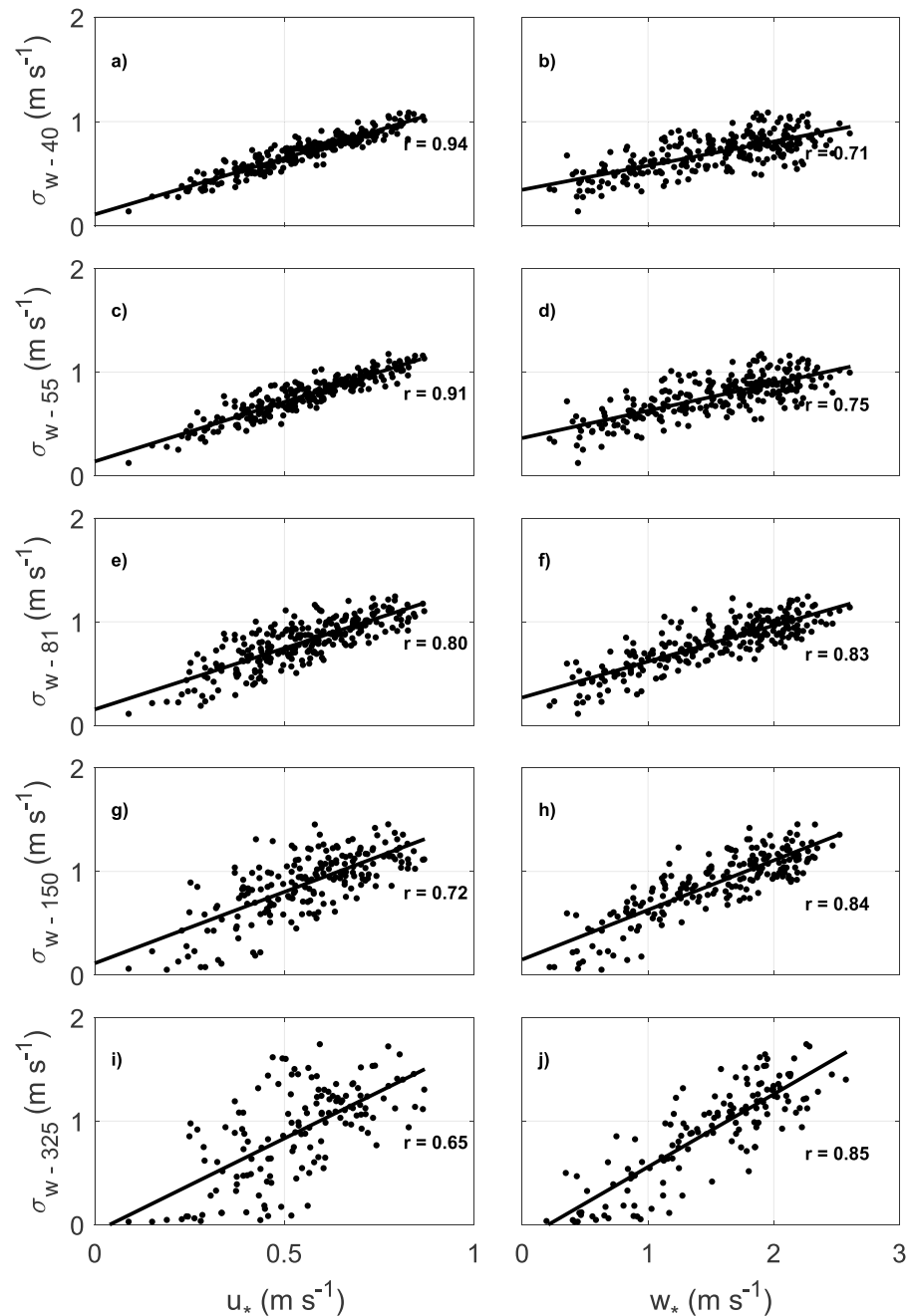


**Figure 2.**  $\sigma_w$  versus  $u_*$  and  $w_*$  at 40 (a,b), 55 (c,d), 81 (e,f), 150 (g,h), and 325 m (i,j).

very close to MOST functions found in the literature. Therefore, neither  $\phi_\tau$  nor  $\phi_w$  are good discriminators between the RSL and the ISL for the ATTO site.

The failure of MOST for scalars in the RSL, on the other hand, is evident. A large scatter and deviation from MOST is observed in the values of  $\sigma_{\theta_v}/\theta_{v*}$  (Figure 1, right side), as also noted by Dias et al. (2009), and by Zahn et al. (2016) and Chor et al. (2017) for the same site. Moreover, the scatter increases continuously with height, with no improvement at an intermediate level that could indicate the presence of an ISL. Other dimensionless statistics,  $\overline{w'\theta'_v}/\overline{w'\theta'_v}|_0$ ,  $\kappa(z-d)\epsilon_e/u_*^3$ , and  $\kappa(z-d)\epsilon_{\theta_v,\theta_v}/(u_*\theta_{v*}^2)$ , for the horizontal virtual heat flux  $\overline{w'\theta'_v}$ , the rate of dissipation of turbulence kinetic energy  $\epsilon_e$ , and the rate of dissipation of virtual temperature semi-variance  $\epsilon_{\theta_v,\theta_v}$  were calculated and compared with standard functions for the ISL (Wyngaard & Coté, 1971;

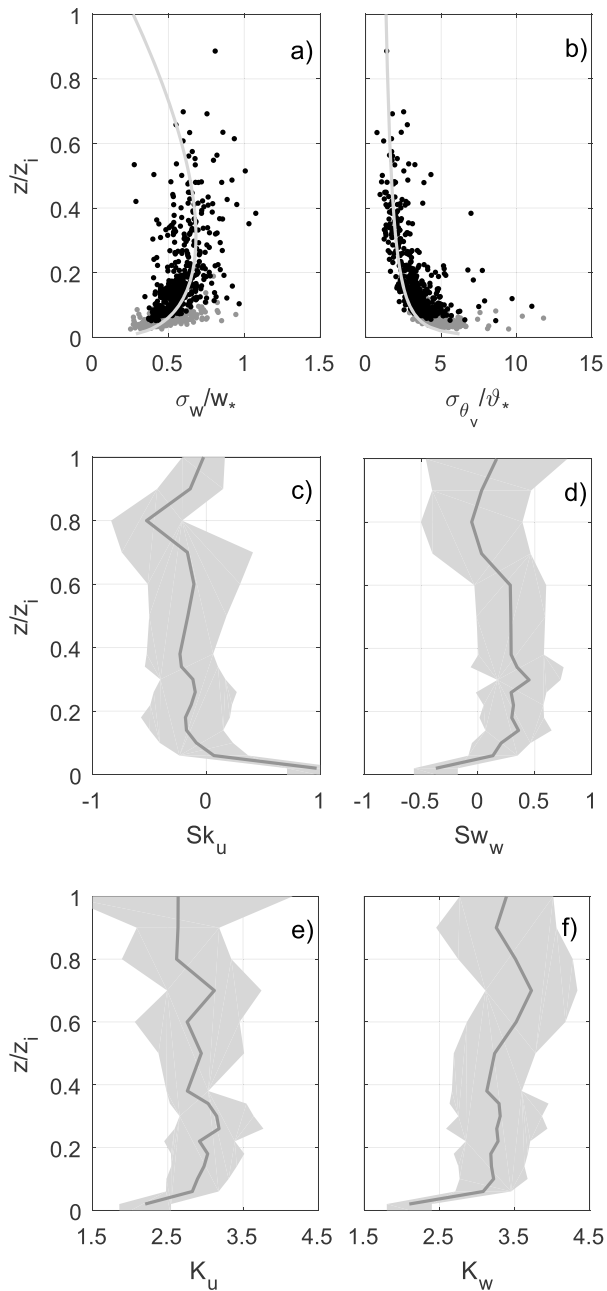


**Figure 3.** Profiles of  $\sigma_w/w_*$  (a) and  $\sigma_{\theta_v}/\vartheta_{v*}$  (b): light gray dots from 40 and 55 m; black dots from 81, 150, and 325 m (the dark gray lines show similarity functions obtained in the mixed layer), and average profiles of  $Sk_u$  (c),  $Sw_w$  (d),  $K_u$  (e), and  $K_w$  (f). The shaded area represents 1 standard deviation around the mean.

Wyngaard, 2010) as well as the predictions of Zilitinkevich (1973) and Kader and Yaglom (1990) with similar results and are shown in Supporting Information S1.

Clearly, MOST scaling does not yield good adjustments at heights 150 and 325 m, as these levels are evidently above the ISL, suggesting a verification of ML scaling. Before that, we note that the plots in Figure 1 may suffer from self-correlation (Hicks, 1981), and further testing of this effect is often required (Andreas & Hicks, 2002; Cava et al., 2008). Because this has already been done at the same site (Chor et al., 2017; Zahn et al., 2016), we are confident that our results are not contaminated by self-correlation. Still, an analysis that is both immune to self-correlation and able to compare SL and ML scaling is the *dimensional* plots of Figure 2, which shows  $\sigma_w$  versus  $u_*$  and  $w_*$ . A similar figure for virtual temperature is given in Supporting Information S1.

In Figure 2, the gradual loss of influence of the SL scale  $u_*$  along with the increasing influence of the ML scale  $w_*$ , is clearly visible.  $\sigma_w$  is very well correlated to  $u_*$  at the two lowest levels ( $r > 0.9$ ), and the correlation coefficient decreases monotonically to 0.65 at 325 m. The opposite trend is observed between  $\sigma_w$  and  $w_*$ , with  $r$  now increasing monotonically from 0.71 to 0.85. For temperature (see Supporting Information S1), the corresponding comparison indicates that both scalings perform equally well at the lower levels but that ML scaling is better at the two upper levels.

#### 4.4. Type-ii Analysis: ML Scaling

The standard deviations  $\sigma_w$  and  $\sigma_{\theta_v}$  divided by  $w_*$  and  $\vartheta_{v*}$  are plotted against  $z/z_i$  in Figures 3a and 3b. Similar analyses are available from wind tunnel and numerical simulations (Amir & Castro, 2011; Johansson et al., 2001; Keirsbulck et al., 2002; Raupach et al., 1980; Zhang et al., 2009) but as far as we know not over the Amazon. In Figures 3a and 3b, the dark gray line indicates the ML similarity functions (Lenschow et al., 1980)

$$\frac{\sigma_w}{w_*} = 1.34 \left( \frac{z}{z_i} \right)^{1/3} \left( 1 - 0.8 \frac{z}{z_i} \right), \quad (4)$$

$$\frac{\sigma_{\theta_v}}{\vartheta_{v*}} = 1.34 \left( \frac{z}{z_i} \right)^{-1/3}. \quad (5)$$

The light gray circles indicate measurements made at 40 and 55 m, and black circles measurements at 81, 150, and 325 m. Except for the two lower levels, (4) fits the data reasonably well (the scatter, although large, is typical of ML measurements; Druihet et al., 1983; Hogan et al., 2009; Johansson et al., 2001; Kaimal et al., 1976 and numerical simulations; Dearnorff, 1974; Ghannam et al., 2017; Moeng, 1984; Yang et al., 2006). At 40 and 55 m, however, the agreement is poor, evidently because ML scaling does not take  $u_*$  into account.

For  $\sigma_{\theta_v}/\vartheta_{v*}$ , agreement with (5) is poor at least up to  $z/z_i = 0.1$ ; the increased variance in this region is typical of scalar behavior in the RSL. Closer to  $z/z_i = 1$ , the scatter increases due to entrainment (Lenschow et al., 1980).

An analysis (not shown) of  $\sigma_u/u_*$  and  $\sigma_w/w_*$  shows that the average  $\sigma_u/u_*$  for  $z/z_i \lesssim 0.07$  never attains the neutral value of 2.5 in the ISL (Garratt, 1994). For the same  $z$  range, both statistics have average values (2.0 and 1.25) that agree with previous measurements in the RSL above the Amazon forest (Dias-Júnior et al., 2015; Kruijt et al., 2000; Santos et al., 2016; Santana et al., 2018). Correlation coefficients between  $w$  and  $u$ , and between  $w$  and  $\theta_v$ , were also plotted against  $z/z_i$ , but it was not possible to discriminate between the RSL

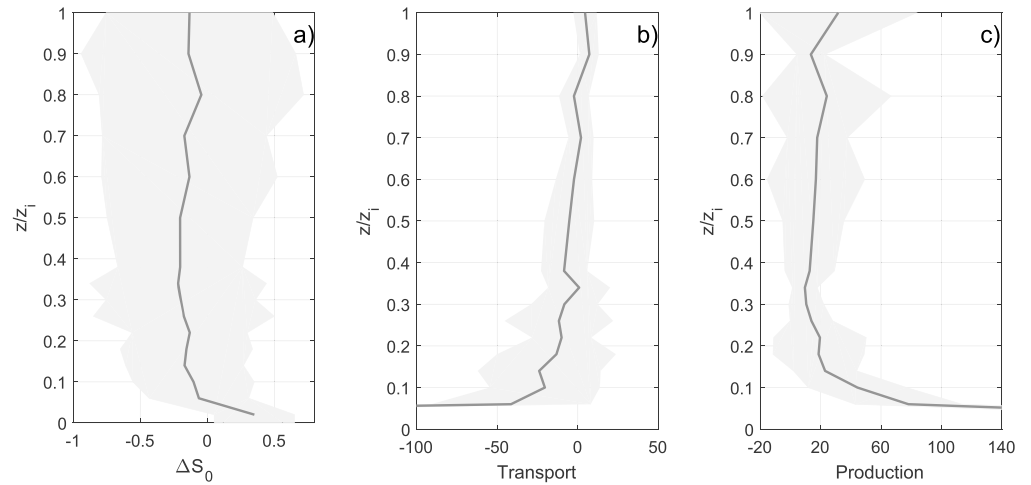


**Figure 4.** The difference  $\Delta S_0$  between sweep and ejection stress contributions for momentum (a), transport term (b), and production term (c) in the turbulence kinetic energy equation. The shaded area represents 1 standard deviation around the mean.

and the ISL. A clear change in the gradient of the correlation coefficients with height, however, again was visible around  $z/z_i = 0.07$ , reinforcing the identification of the top of the SL (see Supporting Information S1 for details).

Figures 3c and 3d show the vertical profiles of the skewnesses  $Sk_u$  and  $Sk_w$ , and Figures 3e and 3f the kurtoses  $K_u$  and  $K_w$  of  $u'$  and  $w'$ , respectively, against  $z/z_i$ . The results confirm previous findings that  $Sk_u > 0$  and  $Sk_w < 0$  above the canopy (Baldocchi & Meyers, 1988; Kruijt et al., 2000; Launiainen et al., 2007; Raupach et al., 1996; Santana et al., 2018). Note that the same signs for these variables are found in the ISL (Katul et al., 1997; Keirsbulck et al., 2002; LeMone, 1990; Schultz & Flack, 2005). In Figures 3c and 3d, the skewness reaches a value of 0 at  $z/z_i \approx 0.07$ , confirming, again, the extent of the SL. For both  $u'$  and  $w'$ , the kurtosis is less than the Gaussian value of 3 up to  $z/z_i \approx 0.07$  as well. Only a two-tiered pattern is evident in the figure.

Quadrant analysis, subsumed by the  $\Delta S_0$  statistics (the contribution to the momentum flux by sweeps minus ejections; Raupach, 1981), is shown in Figure 4a, where  $\Delta S_0 > 0$  in  $z/z_i \leq 0.07$  is typical of the RSL (Poggi et al., 2004; Raupach, 1981; this tendency is also reflected in the signs of  $Sk_u$  and  $Sk_w$ ). In Raupach (1981),  $\Delta S_0 \approx 0$  for  $0.1 \leq \eta \leq 0.3$  ( $\eta$  is roughly equivalent to our  $z/z_i$ ) and becomes markedly negative in the outer region of the boundary layer. Raupach and Thom (1981) consider  $\Delta S_0 \approx 0$  to indicate the ISL. For ATTO's IOP-1,  $\Delta S_0$  is mildly negative from  $z/z_i = 0.07$  to the top of the ML. Finally, in Figures 4b and 4c, we show the dimensionless production and transport terms of the turbulence kinetic energy equation,  $-z_i u' w' \partial \bar{u} / \partial z / u_*^3$  and  $-z_i \partial w' u'_k / \partial z / (2u_*^3)$ . The results agree qualitatively with Figure 5 of Raupach and Thom (1981; from a second-order closure model) and Figure 17 of Finnigan (2000; from observational data) for the RSL, where there are strong mechanical production and negative transport. Again, only a two-tiered structure throughout the ABL is evident.

## 5. Conclusions

An analysis of turbulence statistics from 40 to 325 m was conducted in the Amazon forest, in an attempt to identify an ISL, which usually begins at  $z/h \sim 2.5\text{--}3$  (see Cellier & Brunet, 1992, and references therein). For the Amazon rain forest,  $h \sim 40$  m, and the ISL would not be expected to exist below approximately 100–120 m.

For unstable conditions only, MOST scaling has been tested for  $\sigma_w/u_*$ ,  $\sigma_{\theta_v}/\theta_{v*}$ ,  $\overline{w'\theta'_v}$ ,  $\kappa(z-d)\epsilon_e/u_*^3$  and  $\kappa(z-d)\epsilon_{\theta_v}/(u_*\theta_{v*}^2)$ , and worsens monotonically from 40 to 325 m, indicating no sign of an ISL between the RSL and the convective ML. In an analysis that does not employ  $\zeta$ , the correlation between  $\sigma_w$  and  $u_*$  worsens, and the correlation between  $\sigma_w$  and  $w_*$  improves, monotonically, from 40 to 325 m.

Finally,  $z/z_i$  profiles of several statistics have been analyzed. In all of them, only a two-tiered structure is identifiable, with the lower part  $z/z_i \lesssim 0.07$  always displaying the signature of the RSL, and the remaining upper region showing a behavior that is typical of the ML.

We infer from these analyses that the presence of an ISL is unlikely at the ATTO site. As always, further testing is advisable. In the future, more refined and continuously measured turbulence profiles will be available at the same site, allowing to verify our results more thoroughly: It is still possible that an ISL exist in a narrow region above 100 m; seasonal effects in different periods different may also exist.

The disclosed nonexistence of the ISL in this work has profound implications for the parameterization of scalar fluxes over the Amazon (and possibly other tall forests), since virtually all estimates in use in LES (Basu & Lacser, 2017), weather, and climate models, as well as in studies regarding scalars not easily measured with the eddy covariance method, use MOST in one way or another. Other model estimates, such as precipitation, which is poorly represented in the tropics and is strongly dependent on the latent heat flux, can be impacted as well. This poses new challenges, calling for the development of turbulence theories and methods of flux estimation that are able to cope with this two-layered structure of the Amazonian ABL.

### Acknowledgments

All data used in this work are available in the supporting information. We thank the Max Planck Society and the Instituto Nacional de Pesquisas da Amazônia for continuous support. We acknowledge the support by the German Federal Ministry of Education and Research (BMBF contract 01LB1001A) and the Brazilian Ministério da Ciência, Tecnologia e Inovação (MCTI/FINEP contract 01.11.01248.00) as well as the Amazon State University (UEA), FAPEAM, LBA/INPA, and SDS/CEUC/RDS-405 Uatumã. Further, we would like to thank all colleagues providing technical and logistical support within the ATTO project.

### References

- Alves, E. G., Tota, J., Turnipseed, A., Guenther, A. B., Vega Bustillos, J. O. W., Santana, R. A., & Manzi, A. O. (2018). Leaf phenology as one important driver of seasonal changes in isoprene emission in central Amazonia. *Biogeosciences*, *15*(13), 4019–4032. <https://doi.org/10.5194/bg-15-4019-2018>
- Amir, M., & Castro, I. P. (2011). Turbulence in rough-wall boundary layers: Universality issues. *Experiments in Fluids*, *51*(2), 313–326.
- Andreae, M. O., Acevedo, O. C., Araújo, A., Artaxo, P., Barbosa, C. G. G., Barbosa, H. M. J., & Yáñez Serrano, A. M. (2015). The Amazon Tall Tower Observatory (ATTO): Overview of pilot measurements on ecosystem ecology, meteorology, trace gases, and aerosols. *Atmospheric Chemistry and Physics*, *15*(18), 10,723–10,776. <https://doi.org/10.5194/acp-15-10723-2015>
- Andreas, E. L., & Hicks, B. B. (2002). Comments on “Critical test of the validity of Monin-Obukhov Similarity during convective conditions”. *Journal of the Atmospheric Sciences*, *59*, 2605–2607.
- Baldocchi, D. D., & Meyers, T. P. (1988). Turbulence structure in a deciduous forest. *Boundary-Layer Meteorology*, *43*(4), 345–364.
- Basu, S., & Lacser, A. (2017). A cautionary note on the use of Monin-Obukhov similarity theory in very high-resolution large-eddy simulations. *Boundary-Layer Meteorology*, *163*(2), 351–355.
- Brooks, I. M. (2003). Finding boundary layer top: Application of a wavelet covariance transform to lidar backscatter profiles. *Journal of Atmospheric and Oceanic Technology*, *20*(8), 1092–1105.
- Cava, D., Katul, G. G., Sempreviva, A. M., Giostra, U., & Scrimieri, A. (2008). On the anomalous behaviour of scalar flux-variance similarity functions within the canopy sub-layer of a dense alpine forest. *Boundary-Layer Meteorology*, *128*(1), 33–57.
- Cellier, P., & Brunet, Y. (1992). Flux-gradient relationships above tall plant canopies. *Agricultural and Forest Meteorology*, *58*, 93–117.
- Chor, T. L., Dias, N. L., Araújo, A., Wolff, S., Zahn, E., Manzi, A., & Sörgel, M. (2017). Flux-variance and flux-gradient relationships in the roughness sublayer over the Amazon forest. *Agricultural and Forest Meteorology*, *239*, 213–222. <https://doi.org/10.1016/j.agrformet.2017.03.009>
- Deardorff, J. W. (1974). Three-dimensional numerical study of turbulence in an entraining mixed layer. *Boundary-Layer Meteorology*, *7*, 199–226.
- Dias, N. L., Hong, J., Leclerc, M., Black Nestic, Z., & Krishnan, P. (2009). A simple method of estimating scalar fluxes over forests. *Boundary-Layer Meteorology*, *132*, 401–414. <https://doi.org/10.1007/s10546-009-9408-0>
- Dias-Júnior, C. Q., Marques Filho, E. P., & Sá, L. D. (2015). A large eddy simulation model applied to analyze the turbulent flow above Amazon forest. *Journal of Wind Engineering and Industrial Aerodynamics*, *147*, 143–153.
- Druilhet, A., Frangi, J. P., Guedalia, D., & Fontan, J. (1983). Experimental studies of the turbulence structure parameters of the convective boundary layer. *Journal of Applied Meteorology*, *22*(4), 594–608.
- Finnigan, J. (2000). Turbulence in plant canopies. *Annual Review of Fluid Mechanics*, *32*, 519–571.
- Fisch, G., Tota, J., Machado, L. A. T., Silva Dias, M. A. F., da F. Lyra, R. F., Nobre, C. A., & Gash, J. H. C. (2004). The convective boundary layer over pasture and forest in Amazonia. *Theoretical and Applied Climatology*, *78*(1), 47–59. <https://doi.org/10.1007/s00704-004-0043-x>
- Freire, L. S., & Dias, N. L. (2013). Residual layer effects on the modeling of convective boundary layer growth rates with a slab model using FIFE data. *Journal of Geophysical Research: Atmospheres*, *118*, 12,869–12,878. <https://doi.org/10.1002/jgrd.50796>
- Garratt, J. (1994). *The atmospheric boundary layer* (pp. 316). Cambridge, UK: Cambridge University Press.
- Ghannam, K., Duman, T., Salesky, S. T., Chamecki, M., & Katul, G. (2017). The non-local character of turbulence asymmetry in the convective atmospheric boundary layer. *Quarterly Journal of the Royal Meteorological Society*, *143*(702), 494–507.
- Hicks, B. B. (1981). An examination of turbulence statistics in the surface boundary layer. *Boundary-Layer Meteorology*, *21*, 389–402.
- Hogan, R. J., Grant, A. L., Illingworth, A. J., Pearson, G. N., & O'Connor, E. J. (2009). Vertical velocity variance and skewness in clear and cloud-topped boundary layers as revealed by Doppler lidar. *Quarterly Journal of the Royal Meteorological Society*, *135*(640), 635–643. <https://doi.org/10.1002/qj.413>
- Johansson, C., Smedman, A. S., & Högström, U. (2001). Critical test of the validity of Monin-Obukhov Similarity during convective conditions. *Journal of the Atmospheric Sciences*, *58*, 1549–1566.
- Kader, B. A., & Yaglom, A. M. (1990). Mean fields and fluctuation moments in unstably stratified turbulent boundary layers. *Journal of Fluid Mechanics*, *212*, 637–662.
- Kaimal, J., Wyngaard, J., Haugen, D., Coté, O., Izumi, Y., Caughey, S., & Readings, C. (1976). Turbulence structure in the convective boundary layer. *Journal of the Atmospheric Sciences*, *33*(11), 2152–2169.
- Katul, G., Kuhn, G., Schieldge, J., & Hsieh, C. I. (1997). The ejection-sweep character of scalar fluxes in the unstable surface layer. *Boundary-Layer Meteorology*, *83*(1), 1–26.

- Keirsbulck, L., Labraga, L., Mazouz, A., & Tournier, C. (2002). Surface roughness effects on turbulent boundary layer structures. *Journal of Fluids Engineering-T ASME*, *124*(1), 127–135.
- Kruijt, B., Malhi, Y., Lloyd, J., Norbre, A., Miranda, A., Pereira, M., & Grace, J. (2000). Turbulence statistics above and within two Amazon rain forest canopies. *Boundary-Layer Meteorology*, *94*(2), 297–331.
- Kuhn, U., Andreae, M., Ammann, C., Araújo, A., Brancaleoni, E., & Ciccioli, P. (2007). Isoprene and monoterpene fluxes from Central Amazonian rainforest inferred from tower-based and airborne measurements, and implications on the atmospheric chemistry and the local carbon budget. *Atmospheric Chemistry and Physics*, *7*(11), 2855–2879.
- Launiainen, S., Vesala, T., Mölder, M., Mammarella, I., Smolander, S., Rannik, Ü. G., & Katul, G. (2007). Vertical variability and effect of stability on turbulence characteristics down to the floor of a pine forest. *Tellus B*, *59*(5), 919–936.
- LeMone, M. A. (1990). Some observations of vertical velocity skewness in the convective planetary boundary layer. *Journal of the Atmospheric Sciences*, *47*(9), 1163–1169.
- Lenschow, D. H., Wyngaard, J. C., & Pennell, W. T. (1980). Mean-field and second-moment budgets in a baroclinic, convective boundary layer. *Journal of the Atmospheric Sciences*, *37*, 1313–1326.
- Malhi, Y., McNaughton, K., & Randow, C. V. (2004). Low frequency atmospheric transport and surface flux measurements. In X. Lee, W. Massman, & B. Law (Eds.), *Handbook of micrometeorology* (pp. 101–118). Dordrecht: Kluwer Academic Publishers.
- Mauder, M., & Foken, T. (2004). Documentation and instruction manual of the eddy covariance software package TK2.
- Melfi, S., Spinhirne, J., Chou, S. H., & Palm, S. (1985). Lidar observations of vertically organized convection in the planetary boundary layer over the ocean. *Journal of Applied Meteorology*, *24*(8), 806–821.
- Moeng, C. H. (1984). A large-eddy-simulation model for the study of planetary boundary-layer turbulence. *Journal of the Atmospheric Sciences*, *41*(13), 2052–2062.
- Mölder, M., Grelle, A., Lindroth, A., & Halldin, S. (1999). Flux-profile relationships over a boreal forest—Roughness sublayer corrections. *Agricultural and Forest Meteorology*, *98/99*, 645–658.
- Poggi, D., Porporato, A., Ridolfi, L., Albertson, J. D., & Katul, G. G. (2004). The effect of vegetation density on canopy sub-layer turbulence. *Boundary-Layer Meteorol*, *111*, 565–587.
- Raupach, M. R. (1981). Conditional statistics of Reynolds stress in rough-wall and smooth-wall turbulent boundary layers. *Journal of Fluid Mechanics*, *108*, 363–382.
- Raupach, M. R., Finnigan, J. J., & Brunet, Y. (1996). Coherent eddies and turbulence in vegetation canopies: The mixing-layer analogy. *Boundary-Layer Meteorology 25th Anniversary Volume, 1970–1995* (pp. 351–382). Springer.
- Raupach, M. R., & Thom, A. S. (1981). Turbulence in and above plant canopies. *Annual Review of Fluid Mechanics*, *13*(1), 97–129.
- Raupach, M., Thom, A., & Edwards, I. (1980). A wind tunnel study of turbulent flow close to regularly arrayed rough surfaces. *Boundary-Layer Meteorology*, *18*, 373–397.
- Santana, R. A., Dias-Júnior, C. Q., da Silva, J. T., Fuentes, J. D., do Vale, R. S., Alves, E. G., & Manzi, A. O. (2018). Air turbulence characteristics at multiple sites in and above the Amazon rainforest canopy. *Agricultural and Forest Meteorology*, *260*, 41–54.
- Santos, D. M., Acevedo, O. C., Chamecki, M., Fuentes, J. D., Gerken, T., & Stoy, P. C. (2016). Temporal scales of the nocturnal flow within and above a forest canopy in Amazonia. *Boundary-Layer Meteorology*, *161*(1), 73–98.
- Sawyer, V., & Li, Z. (2013). Detection, variations and intercomparison of the planetary boundary layer depth from radiosonde, lidar and infrared spectrometer. *Atmospheric Environment*, *79*, 518–528.
- Schultz, M., & Flack, K. (2005). Outer layer similarity in fully rough turbulent boundary layers. *Experiments in Fluids*, *38*(3), 328–340.
- Steyn, D. G., Baldi, M., & Hoff, R. (1999). The detection of mixed layer depth and entrainment zone thickness from lidar backscatter profiles. *Journal of Atmospheric and Oceanic Technology*, *16*(7), 953–959.
- Vickers, D., & Mahrt, L. (1997). Quality control and flux sampling problems for tower and aircraft data. *Journal of Atmospheric and Oceanic Technology*, *14*(3), 512–526.
- Viswanadham, Y., Molion, L. C. B., Manzi, A. O., Sá, L. D. A., Filho, V. P. S., André, R. G. B., & dos Santos, R. C. (1990). Micrometeorological measurements in Amazon Forest during GTE/ABLE 2A Mission. *Journal of Geophysical Research*, *95*(D9), 13,669–13,682.
- von Randow, C., Kruijt, B., & Holtslag, A. A. (2006). Low-frequency modulation of the atmospheric surface layer over Amazonian rain forest and its implication for similarity relationships. *Agricultural and Forest Meteorology*, *141*(2–4), 192–207.
- Wang, Z., Cao, X., Zhang, L., Notholt, J., Zhou, B., Liu, R., & Zhang, B. (2012). Lidar measurement of planetary boundary layer height and comparison with microwave profiling radiometer observation. *Atmospheric Measurement Techniques*, *5*(8), 1965–1972.
- Wyngaard, J. C. (2010). *Turbulence in the atmosphere*. Cambridge.
- Wyngaard, J. C., & Coté, O. R. (1971). The budgets of turbulent kinetic energy and temperature variance in the atmospheric surface alayer. *Journal of the Atmospheric Sciences*, *28*, 190–201.
- Yang, B., Raupach, M. R., Shaw, R. H., & Morse, A. P. (2006). Large-eddy simulation of turbulent flow across a forest edge. Part I: Flow statistics. *Boundary-Layer Meteorology*, *120*(3), 377–412.
- Zahn, E., Dias, N. L., Araújo, A., Sá, L. D. A., Sörgel, M., Trebs, I., & Manzi, A. (2016). Scalar turbulent behavior in the roughness sublayer of an Amazonian forest. *Atmospheric Chemistry and Physics*, *16*(17), 11,349–11,366. <https://doi.org/10.5194/acp-16-11349-2016>
- Zhang, J. A., Drennan, W. M., Black, P. G., & French, J. R. (2009). Turbulence structure of the hurricane boundary layer between the outer rainbands. *Journal of the Atmospheric Sciences*, *66*(8), 2455–2467.
- Zilitinkevich, S. (1973). Shear convection. *Boundary-Layer Meteorology*, *3*, 416–423.